Journal of Applied Polymer Science

Poly(L-lactide)/Poly(D-lactide)/Multiwalled Carbon Nanotubes Nanocomposites: Enhanced Dispersion, Crystallization, Mechanical Properties, and Hydrolytic Degradation

Qinglin Dong,[1] Yi Li,[2,3] Changyu Han,[2] Xin Zhang,[1] Kun Xu,[2] Huiliang Zhang,[2] Lisong Dong[2]
[1]Synthetic Resin and Special Fiber Research Center, Changchun University of Technology, Changchun 130012, China
[2]Key Laboratory of Polymer Ecomaterials, Changchun Institute of Applied Chemistry, Chinese Academy of Sciences, Changchun 130022, China
[3]College of Material Science and Engineering, Jilin Jianzhu University, ChangChun 130118, China
Correspondence to: C. Han (E-mail: cyhan@ciac.jl.cn) or H. Zhang (E-mail: hlzhang@ciac.jl.cn)

ABSTRACT: Biodegradable stereocomplex-type poly(L-lactide) (PLLA)/poly(D-lactide) (PDLA)/multiwalled carbon nanotubes (MWCNTs) nanocomposites are prepared via simple melt blending method at PDLA loadings from 5 to 20 wt %. Formation of the stereocomplex crystals in the nanocomposites is confirmed by the phase transition in the differential scanning calorimetric profiles. Field emission scanning electron microscopy observation indicates that MWCNTs are nicely dispersed in the PLLA/PDLA/MWCNTs ternary blends with 20 wt % PDLA loading due to the increased shear stress in the melt-compounding with presence of PDLA. The overall crystallization rates are faster in the PLLA/PDLA/MWCNTs nanocomposites than in PLLA/MWCNTs nanocomposite; however, the crystallization mechanism and crystal structure of these nanocomposites remain unchanged despite the presence of PDLA. The storage modulus above glass transition temperature has been apparently improved in the PLLA/PDLA/MWCNTs nanocomposites with respect to PLLA/MWCNTs nanocomposite. It is interesting to find that the hydrolytic degradation rates have been enhanced obviously in the PLLA/PDLA/MWCNTs nanocomposites than in PLLA/MWCNTs nanocomposite, which may be of great use and importance for the wider practical application of PLLA/MWCNTs nanocomposites. © 2013 Wiley Periodicals, Inc. J. Appl. Polym. Sci. 130: 3919–3929, 2013

KEYWORDS: biodegradability; crystallization; mechanical properties

Received 4 April 2013; accepted 15 June 2013; Published online 2 July 2013
DOI: 10.1002/app.39667

INTRODUCTION

Poly(L-lactide) (PLLA) has attracted much attention because it is biomass-derived, biodegradable, biocompatible, and nontoxic to the environment and human body. Recent innovation on the production process has lowered significantly the production cost, which further stimulates the studies on its property and potential applications.[1–4] However, the poor thermal stability with low levels of heat deflection temperature, gas barrier properties, and low impact resistance of PLLA greatly limit its further development and industrial applications. Due to slow crystallization rate, PLLA is generally amorphous after conventional extrusion or injection molding. Since PLLA is a semicrystalline polymer, controlled crystallization rate and morphology are extremely important in determining its physical and chemical properties.[5]

Poly(lactic acid) (PLA) has three enantiomeric forms: L-lactic acid (PLLA), D-lactic acid (PDLA), and racemic-lactic acid (PDLLA), showing various properties.[6] A special crystalline structure termed stereocomplex based on $CH_3 \ldots C{=}O$ interactions of stereoselective van der Waals forces can be formed by the melt blending, solution casting, or supercritical fluid methods when mixing PLLA and PDLA with identical chemical composition but different steric structures.[7] The pure PLLA usually crystallizes in a form with a 10_3 helical chain conformation, while the stereocomplex-PLA possesses a triclinic unit cell with a 3_1 helical chain conformation.[8] This stereocomplex type poly(lactic acid) (sc-PLA) showed its T_m at 230°C, which is about 50°C higher than that of pure PLLA or PDLA, so that sc-PLA should accordingly have better thermal and mechanical properties, and higher hydrolytic stability than PLLA or PDLA. Since the first report by Ikada et al., the influences of the homopolymer molecular weight, blending ratio (equimolar and non-equimolar), blending condition, and optical purity on the formation and properties of stereocomplexes have been well investigated.[9–19]

Moreover, during the past few years, various nanofillers such as layered silicate (clay), silica, multiwalled carbon nanotubes (MWCNTs), and polyhedral oligomeric silsesquioxanes have

been widely used for the preparation of nanocomposites with different types of environmentally friendly polymer resins.[20–23] However, nanocomposites based on PLLA and MWCNTs have attracted great interest in today's materials research, because these substances can significantly enhance the nanocomposite properties especially when compared with neat PLLA.[24–27] These improvements can include high moduli, increased strength, increased electronic conductivity and increased rate of crystallization, and control of biodegradability.[24–27]

It should be noted that stereocomplex-type PLLA/MWCNTs nanocomposites have not attracted much more consideration yet. In a very recent work, equimolar stereocomplex-type nanocomposites based on PLLA and MWCNTs were prepared by a directly melt mixing process.[17] The electrical conductivities were greatly improved by the formation of stereocomplex compared to that of PLLA/MWCNTs composites at same MWCNTs content. The X-ray diffraction, non-isothermal, and isothermal crystallization results showed that the formation of stereocomplex greatly increased the crystallinity of the composites, meanwhile MWCNTs acted as heterogeneous nucleating agent, which significantly accelerated the nucleation and spherulite growth. However, to the best of our knowledge, the studies on the non-equimolar stereocomplex-type nanocomposites based on PLLA and MWCNTs by simple melt processing have not been reported yet. Therefore, in this work, stereocomplex-type nanocomposites based on PLLA and MWCNTs were prepared by simple melt blending of asymmetric PLLA/PDLA with different amounts of PDLA for the first time. The influences of *in situ* formed stereocomplex crystals during melt processing on the morphology, crystallization, mechanical properties, and hydrolytic degradation of PLLA/MWCNTs nanocomposites were studied in detail with various techniques. It is expected that the research reported herein is of great help for further improving of the crystallization behaviors, mechanical properties, and hydrolytic degradation of PLLA/MWCNTs nanocomposites and for future applications.

MATERIALS AND METHODS

Materials

PLLA (4032D) was a commercial product of NatureWorks. It exhibited a weight-average molecular weight (M_w) of 207,000, polydispersity of 1.73. D-isomer content of PLLA is approximately 2.0%. PDLA were synthesized by the ring-opening polymerization of D-lactide using tin octanoate as a catalyst. It exhibited a M_w of 110,000, polydispersity of 1.92. Pristine MWCNTs without any surface treatment were purchased from Chengdu Organic Chemicals, the Chinese Academy of Sciences R&D center for Carbon Nanotubes. The MWNTs (purity > 95%) has an outside diameter of about 8 nm, inside diameter of 2–5 nm and length of 10–30 um. PLLA, PDLA, and MWCNTs were dried in a vacuum oven at 80°C for 2 days before use.

Formation of Nanocomposites

PLLA/PDLA/MWCNTs nanocomposites were prepared using a Haake rheomix 600 internal mixer. The melt compounding of PLLA, PDLA, and MWCNTs was performed at 180°C for 5 min, the rotor speed was 60 rpm, and the total mixing weight per batch was about 60 g. For comparison, neat PLLA and PLLA/MWCNTs were treated with the same procedure, respectively. The contents of MWCNTs were fixed at 1.0 wt % based on total blend weight. The contents of PDLA were 5, 10, and 20 wt % based on per hundreds weight of PLLA. The samples are abbreviated as PLLA/PDLA*x*/MWCNTs, where *x* is the content of PDLA. For instance, PLLA/PDLA5/MWCNTs refers to nanocomposite based on 5 wt % PDLA and 1.0 wt % MWCNTs. Then, to attain the film samples with thickness of 0.2–1.0 mm for characterization, the melt compounding samples were hot-pressed under a pressure of 10 MPa at 190°C after melting for 2 min, followed by a quenching in liquid nitrogen. Stereocomplex crystallites formed in the blends stayed unmelted at 190°C and embedded in the PLLA matrix. All test specimens were conditioned for 3 days at 23°C and 50% RH prior to testing and characterization.

Gel Permeation Chromatography

The molecular weight parameters of various samples were measured using gel permeation chromatography (GPC) with a Waters 410 GPC instrument equipped with two Waters Styragel columns (HT6E and HT3) and a differential refractometer detector. Measurements were performed at 25°C and at a flow rate of 1.0 mL min^{-1} using chloroform as eluent. The molecular weight was calibrated according to polystyrene standards (Polyscience).

Differential Scanning Calorimetry

Thermal analysis was performed using a TA Instruments differential scanning calorimetry (DSC) Q20 with a Universal Analysis 2000. All operations were performed under nitrogen purge, and the weight of the samples varied between 5 and 8 mg. In the case of the samples quenched in liquid nitrogen, the samples were heated from 20 to 250°C at a rate of 5°C/min. For isothermal melt crystallization of neat PLLA and its nanocomposites, the samples were heated to 190°C at 50°C/min, held for 2 min to erase any thermal history, then cooled to the desired crystallization temperature (T_c) at 45°C/min, and held for a period of time until the isothermal crystallization was complete. The exothermal traces were recorded for the later data analysis.

Field Emission Scanning Electron Microscopy

The morphology of the surface of various samples was observed using an field emission scanning electron microscopy (ESEM; XL30 ESEM FEG, FEI) at an accelerating voltage of 10 kV. The surface was coated with a thin layer of gold prior to the measurement.

Polarized Optical Microscope

A polarized optical microscope (POM; OlympusBX51) equipped with a temperature controller (Linkam THMS 600) was used to investigate the spherulitic morphology of neat PLLA and its nanocomposites. The samples were first annealed at 190°C for 2 min to erase any thermal history and then cooled to 130°C at 45°C/min and held for 2 h.

Wide-Angle X-Ray Diffraction

Wide-angle X-ray diffraction (WAXD) experiments were performed on a D8 advance X-ray diffractometer (Bruker, Germany) at room temperature in the range of 2–40° with a

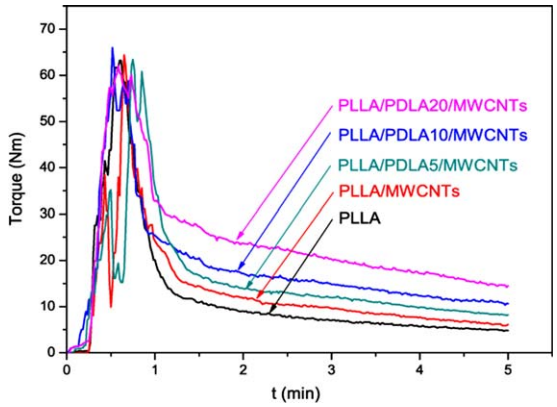

Figure 1. Torque vs. time for the melting of neat PLLA, PLLA/MWCNTs, and PLLA/PDLA/MWCNTs nanocomposites. [Color figure can be viewed in the online issue, which is available at wileyonlinelibrary.com.]

scanning rate of 4°/min. The Cu Kα radiation (λ = 0.15418 nm) source was operated at 40 kV and 200 mA.

Dynamic Mechanical Analysis

Dynamic mechanical analysis (DMA) was performed on the samples of 20 × 4 × 1 mm^3 in size using a dynamic mechanical analyzer from Rheometric Scientific under tension mode in a temperature range of 0 to 125°C at a frequency of 1 Hz and 3°C/min.

Hydrolytic Degradation

The hydrolytic degradation of neat PLLA and its nanocomposites samples of 1 × 1 cm^2 in size was carried out in sodium hydroxide (NaOH) solution (pH = 13) at 37°C. The thickness of the films was around 0.2 mm. The degradation of neat PLLA and its nanocomposites was determined by the variation of weight loss with degradation time. The weight loss coefficient W_{loss} (%) = 100 × (W_0 − $W_{t\text{-dried}}$)/W_0, where W_0 is the initial weight and $W_{t\text{-dried}}$ is the weight of sample subjected to hydrolytic degradation for time t and drying in vacuum. Three specimens were used to obtain the average W_{loss} values. Moreover, the hydrolytic degradation rate R was determined by the following relationship, that is, $R = dW_{loss\text{-}t}/dt$, where $W_{loss\text{-}t}$ is the weight loss and t is the exposed time in NaOH solution.

RESULTS AND DISCUSSION

Stereocomplex Formation

Figure 1 shows the torque change with time during polymer melting or blending performed in a Haake torque rheometer. In Figure 1, the torque of each formulation shows a sharp and strong peak at about 0.5–1 min, which was attributed to the melting process of the PLLA and/or PDLA pellets and then became flat. For the mixing of PLLA/MWCNTs binary blend, a slight increase of torque after the melting of the pellets is noted compared with neat PLLA, which may be ascribed to the strengthening effect of MWCNTs on PLLA melt. After melt processing, the molecular weights parameters of neat PLLA and PLLA/MWCNTs samples were investigated by GPC. The M_w values of, melt-processed PLLA and PLLA/MWCNTs samples are 195,000 and 191,000 with M_w/M_n values of 1.76 and 1.74, respectively. The molecular weight parameters characterization confirms

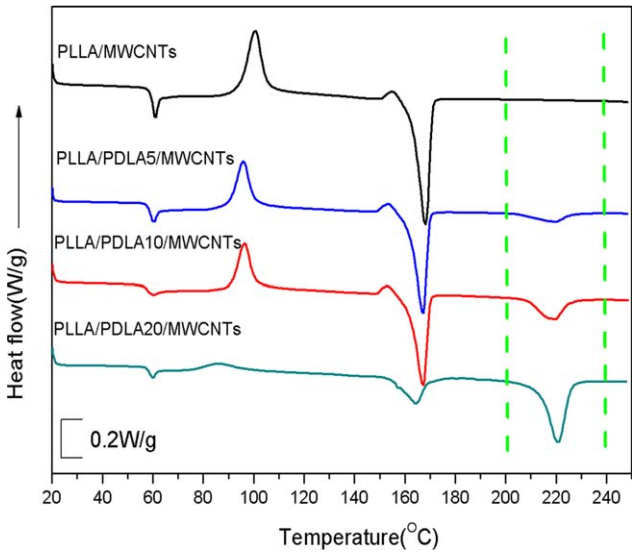

Figure 2. DSC traces obtained on the quenched nanocomposites containing various content of PDLA at a heating rate of 5°C/min. [Color figure can be viewed in the online issue, which is available at wileyonlinelibrary.com.]

that, under processing conditions used in this work, melt blending of PLLA and PLLA with MWCNTs does not induce any dramatic drop of PLLA weight-average molar mass by thermal degradation or hydrolysis of the polyester chains. For the mixing of PLLA/PDLA/MWCNTs ternary blends, an obviously increment in torque after the melting of the pellets is observed. Furthermore, the corresponding torque for the PLLA/PDLA/MWCNTs ternary blends becomes higher with an increase in the PDLA loading, indicating the stereocomplex forms *in situ* in the PLLA/PDLA/MWCNTs ternary blends. As the stereocomplex forms in the PLLA/PDLA/MWCNTs nanocomposites, PLLA homopolymer chains can possibly become tethered to or stuck in the stereocomplex crystallites, thus reducing chain mobility. When large amounts of PDLA are present (20 wt %), more tethering sites are formed, and PLLA homopolymer chains may be tethered at multiple junctures.[12] This will significantly hinder chain mobility, increase the melt viscosity, resulting in an enhanced torque during melt blending. In other words, after incorporation of PDLA, the intensity of shear during melt blending of PLLA/MWCNTs nanocomposites has been enhanced, which will contribute to the improved dispersion of MWCNTs in the nanocomposites as discussed later on.

Formation of the stereocomplex crystals in the blends was further confirmed by DSC. DSC traces obtained on the quenched samples containing various content of PDLA at a heating rate of 5°C/min are given in Figure 2. In all the samples, the glass transition, the cold crystallization, and melting peak from the PLLA homopolymer are present around 60°C, 100°C, and 168°C, respectively, while the stereocomplex melting peak is present around 218°C as reported in the literature.[16] The area of the melting endotherm for the stereocomplex crystals increased as the amount of PDLA in the blend increased showing that the initial composition of the blend can be used to control the amount of stereocomplex in the final material.

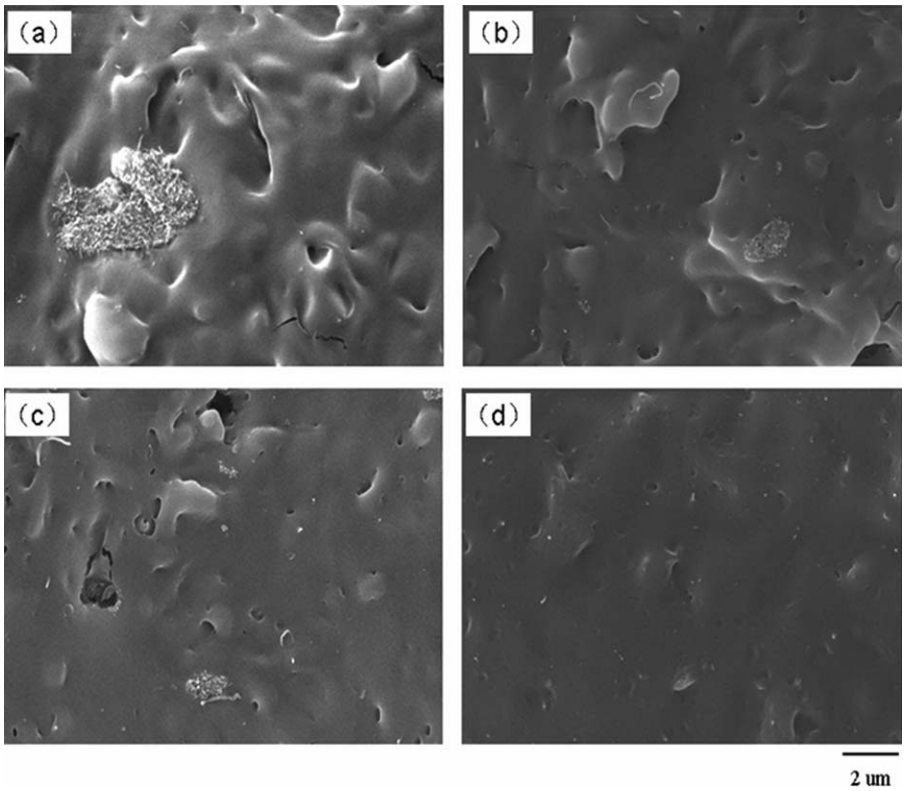

Figure 3. ESEM images of various nanocomposites: (a) PLLA/MWCNTs, (b) PLLA/PDLA5/MWCNTs, (c) PLLA/PDLA10/MWCNTs, and (d) PLLA/PDLA20/MWCNTs.

Morphology and Dispersion of MWCNTs in the PLLA Matrix

It is well known that the dispersion of MWCNTs in the polymer matrix plays a dominant role of influencing the physical and chemical properties of biodegradable polymers. The fracture surface morphology of PLLA/MWCNTs and PLLA/PDLA/MWCNTs nanocomposites samples was studied with ESEM first. Figure 3 shows the ESEM images of PLLA/MWCNTs nanocomposite and PLLA/MWCNTs nanocomposites containing 5–20 wt % PDLA. The random dispersed bright dots and lines are the ends of the broken carbon nanotubes. For PLLA/MWCNTs nanocomposite, severe aggregation of MWCNTs with dimensions around 4 um is observed on the morphology as seen in Figure 3(a). The presence of electrostatic and van der Waals interactions lead to apparent aggregation of pristine MWNTs. Very similar dispersions of MWCNTs were also observed in PLLA/MWCNTs nanocomposites prepared by solution and coagulation method.[22] However, For PLLA/PDLA5/MWCNTs and PLLA/PDLA10/MWCNTs samples, the dispersions of MWCNTs are obviously improved. The aggregation of MWCNTs with dimensions around 2 um is observed. It should be noted that for PLLA/PDLA20/MWCNTs sample, a fine dispersion of MWCNTs can be observed in the PLLA matrix. The dispersion of nanoparticles in a polymer matrix has been reported to be dependent on the shear stresses exerted on the nanoparticles during melt mixing.[28] The shear stress can overwhelm the electrostatic and van der Waals' interactions in the fillers and lead to the breakup of the filler agglomerates. After incorporation of PDLA, the intensity of shear during melt blending of PLLA/MWCNTs nanocomposites has been increased as evidenced from Figure 1. This increased shear stress effectively overwhelms the electrostatic and van der Waals' interactions in the MWCNTs and leads to a fine dispersion of MWCNTs in PLLA matrix. Introduction of PDLA during melt compounding provides a fine dispersion of pristine MWCNTs in the PLLA matrix, which should be of great importance in studying the structure and properties relationship of biodegradable polymer/MWCNTs nanocomposites.

Isothermal Melt Crystallization

It is of great interest to investigate the addition of PDLA on the crystallization of PLLA/MWCNTs nanocomposites. As introduced in the Experimental Section, the overall isothermal crystallization kinetics of neat PLLA, PLLA/MWCNTs, and PLLA/PDLA/MWCNTs nanocomposites was studied with DSC in a temperature range from 130 to 140°C. Figure 4(a) shows the plots of relative crystallinity against crystallization time at 130°C. It can be seen from Figure 4(a) that all these curves have the similar sigmoid shape. The corresponding crystallization time for the PLLA/MWCNTs nanocomposite is shorter than that of neat PLLA, indicating a nucleation effect of MWCNTs as reported previously.[22] Actually, both surface chemistry and dispersion of MWCNTs play important roles in affecting the crystallization behaviors of polymer/MWCNTs nanocomposites.[22] It should be noted that the corresponding crystallization time for the PLLA/PDLA/MWCNTs nanocomposites becomes obviously shorter after incorporation of PDLA

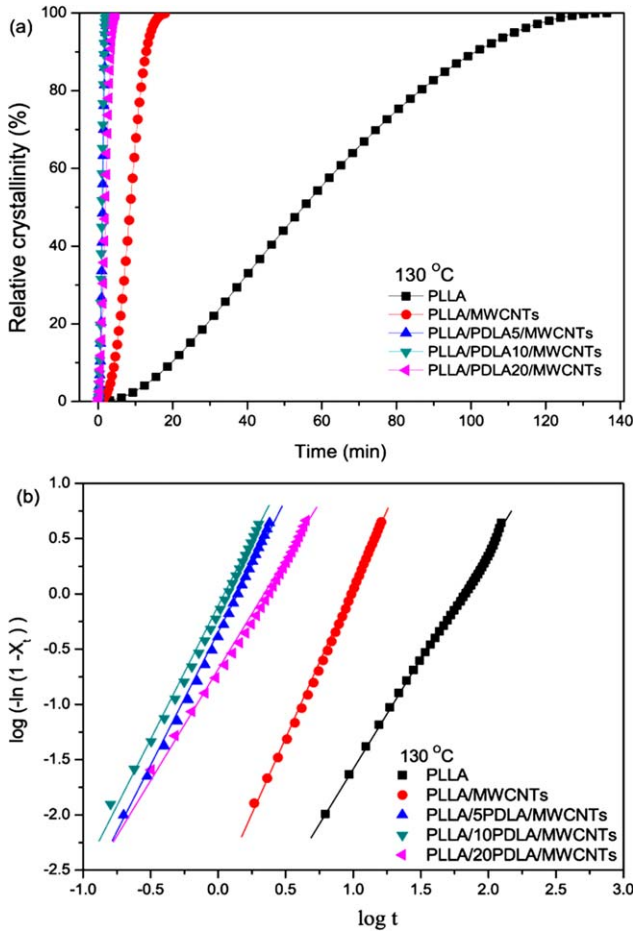

Figure 4. (a) Variation of relative crystallinity with crystallization time for neat PLLA and various nanocomposites at 130°C and (b) the related Avrami plots. [Color figure can be viewed in the online issue, which is available at wileyonlinelibrary.com.]

loading. For example, it took PLLA/MWCNTs sample almost 18 min to complete crystallization at 130°C; however, for the PLLA/PDLA5/MWCNTs, PLLA/PDLA10/MWCNTs, and PLLA/PDLA20/MWCNTs nanocomposites, the time required to finish crystallization became only around 8, 4, and 5 min, respectively. It is clear that the addition of PDLA greatly enhances the isothermal melt crystallization of PLLA/MWCNTs nanocomposites.

The Avrami equation is frequently used to analyze the isothermal crystallization kinetics of polymers, according to which the relative degree of crystallinity X_t dependent crystallization time t can be expressed as,[29,30]

$$1-X_t=\exp(-kt^n) \tag{1}$$

where X_t is the relative degree of crystallinity, n is the Avrami exponent depending on the nature of nucleation and growth geometry of the crystals, and k is the overall rate constant associated with both nucleation and growth contributions. The linear form of eq. (1) can be expressed as follows:

$$\mathrm{Log}[-\ln(1-X_t)]=\log k+n\log t \tag{2}$$

The Avrami parameters n and k can be obtained from the slopes and the intercepts, respectively.

Table I. Parameters of PLLA and Various Nanocomposites From Avrami Equation

Sample	T_c (°C)	n	K (min^{-n})
PLLA	130	2.1	2.50×10^{-4}
	135	2.4	1.92×10^{-5}
	140	2.2	2.18×10^{-5}
PLLA/MWCNTs	130	2.7	2.27×10^{-3}
	135	2.8	2.26×10^{-4}
	140	2.3	2.95×10^{-4}
PLLA/PDLA5/MWCNTs	130	2.6	0.45
	135	2.6	0.20
	140	2.6	5.57×10^{-2}
PLLA/PDLA10/MWCNTs	130	2.4	0.73
	135	2.6	0.24
	140	2.6	7.37×10^{-2}
PLLA/PDLA20/MWCNTs	130	2.0	0.19
	135	2.0	0.12
	140	2.1	6.98×10^{-2}

In the case of the DSC experiment, X_t at t is defined as the ratio of the area under the exothermic curve between the onset crystallization time and t to the whole area under the exothermic curve from the onset crystallization time to the end crystallization time. Figure 4(b) shows the Avrami plots of neat PLLA, PLLA/MWCNTs, and PLLA/PDLA/MWCNTs nanocomposites crystallized at 140°C as an example, from which the Avrami parameters n and k can be obtained from the slopes and the intercepts, respectively. The obtained Avrami parameters of neat PLLA, PLLA/MWCNTs, and PLLA/PDLA/MWCNTs nanocomposites are summarized in Table I for comparison, from which it can be seen that the average values of n are around 2.3 for neat PLLA and 2.5 for its nanocomposites at the investigated T_cs. The almost unaltered n values suggest that crystallization mechanism of PLLA in the PLLA/MWCNTs and PLLA/PDLA/MWCNTs nanocomposites may not change. Moreover, the values of k are also listed in Table I.

The crystallization half-time ($t_{0.5}$), the time required to achieve 50% of the final crystallinity of the samples, is introduced for comparing the overall crystallization rates. The value of $t_{0.5}$ is calculated by the following equation:

$$t_{0.5}=\left(\frac{\ln 2}{k}\right)^{1/n} \tag{3}$$

The crystallization rate can thus be easily described by the reciprocal of $t_{0.5}$. Figure 5 panels a and b illustrate the variations of $t_{0.5}$ and $1/t_{0.5}$ with T_c for neat PLLA, PLLA/MWCNTs, and PLLA/PDLA/MWCNTs nanocomposites, respectively, from which the effects of T_c and the PDLA loading on the variation of overall crystallization rate can be obtained clearly. As shown in Figure 5, the values of $t_{0.5}$ increase while the values of $1/t_{0.5}$ decrease with increasing T_c for both neat PLLA and its nanocomposites. Such variations indicate that the overall isothermal crystallization rate decreases with increasing T_c. In addition, the

Applied Polymer SCIENCE

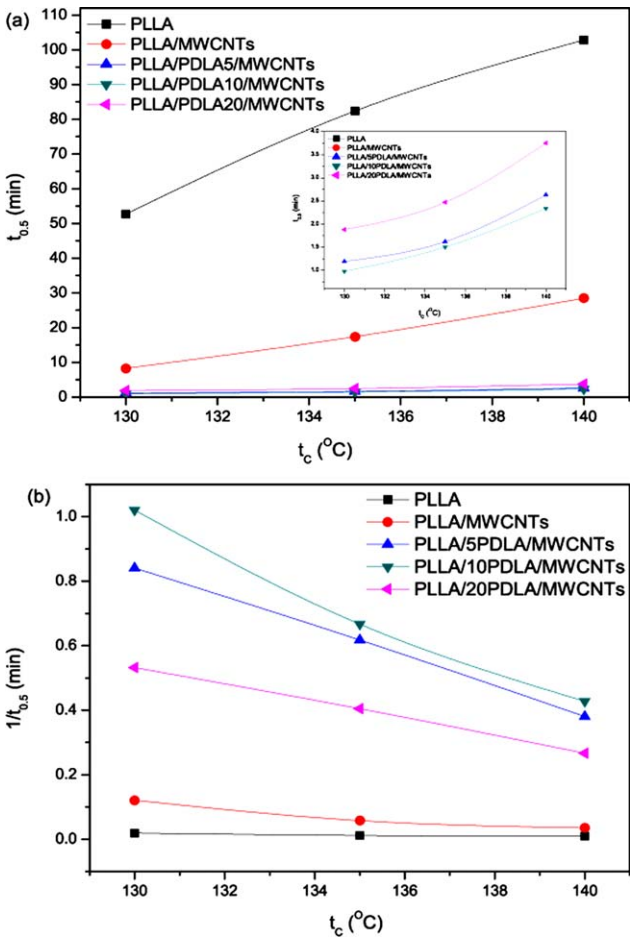

Figure 5. Temperature dependences of (a) $t_{0.5}$ and (b) $1/t_{0.5}$ for neat PLLA and various nanocomposites at various T_cs. [Color figure can be viewed in the online issue, which is available at wileyonlinelibrary.com.]

values of $t_{0.5}$ for PLLA/PDLA/MWCNTs nanocomposites are smaller than those of PLLA/MWCNTs at a given T_c, indicating again that the crystallization process of PLLA/MWCNTs nanocomposites is accelerated after incorporation of PDLA, which should be due to the heterogeneous nucleation agent effect of *in situ* formed stereocomplex crystals.[16] The DSC results reported herein are consistent with the spherulitic morphology and growth studies in the following section. It should be noted that the $1/t_{0.5}$ value first increases and then decreases with increasing the PDLA loading and exhibits the maximum value in the PLLA/PDLA10/MWCNTs sample, suggesting that the PDLA loading has a significant effect of accelerating the crystallization of PLLA/MWCNTs nanocomposites. Therefore, it is necessary to discuss the effect of the presence of PDLA and their loadings on the crystallization behavior of PLLA/MWCNTs nanocomposites. The overall crystallization process of polymers generally involves both nucleation and growth. The stereocomplex crystals formed in the nanocomposites play two different or competing roles in affecting the crystallization process of PLLA/MWCNTs nanocomposites. On the one hand, stereocomplex crystals served as nucleating agent accelerate the isothermal crystallization of PLLA/MWCNTs nanocomposites as discussed earlier. On the other hand, during crystallization process, the polymer chains must overcome certain energy barriers to diffuse and attach onto the growing front of a crystal. The presence of stereocomplex crystals may act as a physical cross-linking point to restrict the movement of chain segments and hinder the crystal growth process by imposing the constrains on the surrounding polymer chains especially when they have good interactions with polymer chains. At PDLA contents less than 10 wt %, the crystallization of PLLA/MWCNTs nanocomposites is enhanced with increasing the PDLA loading because the nucleation effect induced by the stereocomplex crystals is predominated. With further increasing the PDLA content up to 20 wt %, although stereocomplex crystals may provide more nucleation sites, the presence of more stereocomplex crystals must impose a much more significant confinement effect on the crystal growth of PLLA/MWCNTs nanocomposites, which decreases the overall crystallization rate. A similar confinement effect on melt crystallization and cold crystallization in asymmetric PLLA/PDLA blends prepared by solution casting was also observed in previous work.[12,19]

Spherulitic morphology of neat PLLA, PLLA/MWCNTs, and PLLA/PDLA/MWCNTs nanocomposites was studied with POM. Figure 6 shows the spherulitic morphology of neat PLLA, PLLA/MWCNTs, and PLLA/PDLA/MWCNTs nanocomposites isothermally crystallized at 130°C for 2 h. It can be seen from Figure 6(a) that the well-developed spherulites grow to a size of about 50 um in diameter, and the boundaries can be seen clearly for neat PLLA and PLLA/MWCNTs samples. Figure 6 panels c, d, and e illustrate the POM images of the nanocomposites with the PDLA loading from 5 to 20 wt %. The presence of PDLA in the PLLA/MWCNTs nanocomposites resulted in smaller size of spherulites and obscurer spherulites boundaries. However, the content of PDLA in the nanocomposites did not show obvious effect on the morphology of spherulites.

WAXD experiments were performed to investigate the effect of the addition of PDLA on the crystal structure in the PLLA/PDLA/MWCNTs nanocomposites. PLLA can crystallize in α, β, and γ forms. The most common polymorph of PLLA is the α form, which is believed to grow under the normal conditions such as the melt, cold, or solution crystallization.[31] Recently, a new crystal modification α' has also been found.[32,33] The formation of the metastable α'-form crystals of PLLA is kinetically preferential, while that of the thermally stable α-form crystals is thermodynamically favored. It has been found that the disorder α' and order α phases are formed at low ($T_c < 100$°C) and high ($T_c > 120$°C) temperatures, respectively. In this work, the samples were first pressed into films with a thickness of around 0.2 mm at 190°C and then transferred into a vacuum oven at 130°C for 24 h; therefore, neat PLLA, PLLA/MWCNTs, and PLLA/PDLA/MWCNTs nanocomposites should crystallize in α form. In Figure 7, neat PLLA, PLLA/MWCNTs, and PLLA/PDLA/MWCNTs nanocomposites exhibit three main characteristic diffraction peaks at around 15.0°, 16.8°, and 19.2°, corresponding to (010), (200), and (203), respectively.[4] Moreover, PLLA/PDLA/MWCNTs nanocomposites also exhibit nearly the same diffraction peaks at the same locations, indicating that incorporating with PDLA does not modify the crystal structure of these nanocomposites. In addition, the characteristic

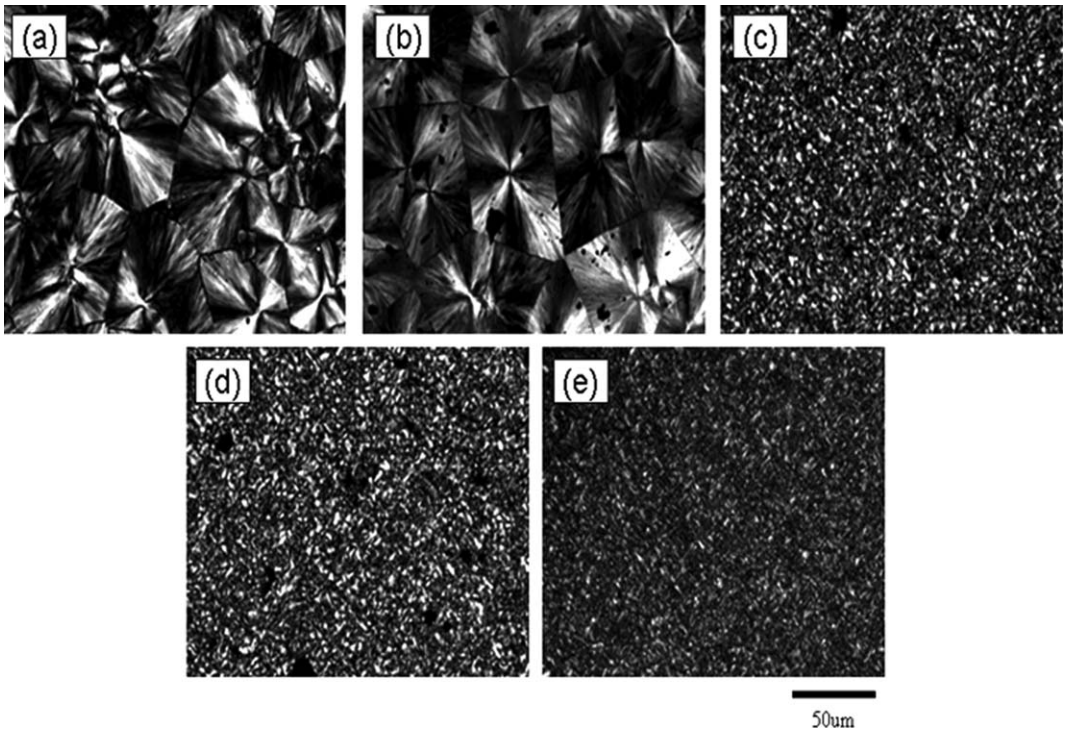

Figure 6. POM images of neat PLLA and various nanocomposites (with the same tool bar): (a) neat PLLA, (b) PLLA/MWCNTs, (c) PLLA/PDLA5/MWCNTs, (d) PLLA/PDLA10/MWCNTs, and (e) PLLA/PDLA20/MWCNTs.

diffraction peaks of stereocomplex crystals at 2θ values of 12, 21, and 24° appear in the PLLA/PDLA/MWCNTs nanocomposites,[17] suggesting that stereocomplex crystals exist as the separate crystals are able to crystallize when they are dispersed in the PLLA matrix. In brief, the crystal structure remains unchanged despite the addition of PDLA in the PLLA/MWCNTs nanocomposites.

DMA

DMA measures the response of a given material to a cyclic deformation (here in tension–torsion mode) as a function of the temperature. DMA results are expressed by two main parameters: (a) the storage modulus (E'), corresponding to the elastic response to the deformation, and (b) tan δ, that is the ratio of loss modulus to storage modulus, useful for determining the occurrence of molecular mobility transitions such as the glass transition temperature (T_g).

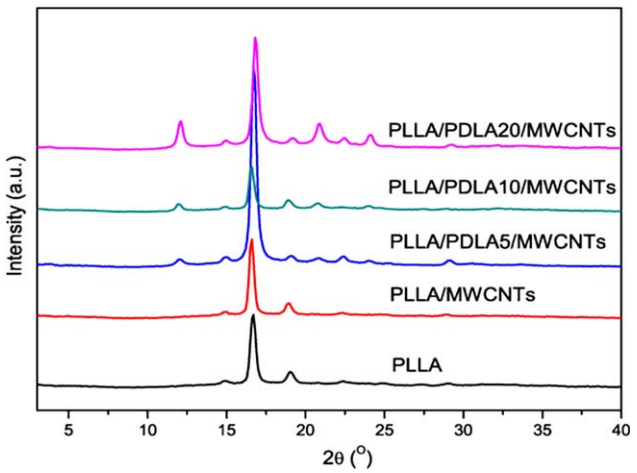

Figure 7. WAXD patterns of neat PLLA and various nanocomposites. [Color figure can be viewed in the online issue, which is available at wileyonlinelibrary.com.]

Here, DMA analysis has been studied to track the temperature dependence of storage modulus and determine the glass transition temperature on the various nanocomposites formation. Figure 8 panels a and b show the temperature dependence of storage modulus (E') and tan δ of neat PLLA, PLLA/MWCNTs, and PLLA/PDLA/MWCNTs nanocomposites, respectively. From Figure 8(a), the storage modulus (E') of PLLA at room temperature was about 3 GPa, in agreement with the value as reported previously.[34] The glass transition of PLLA started at about 60°C, and the storage modulus accordingly decreased sharply. Then, the cold crystallization happened at around 90°C, and as the result of crystallization, the storage modulus increased. Similar characteristic temperature dependence of E' for other nanocomposites is also observed. However, a considerable increase of the storage modulus is found after the incorporation of PDLA at temperature above the glass state (80–90°C), indicating that the addition of PDLA induces a reinforcement effect. For example, the value of E' is only 4.0, 5.2 MPa for neat PLLA and PLLA/MWCNTs nanocomposites at 82°C, respectively, which increases to around 14.0, 21.9, and 92.6 MPa, respectively, with increasing the PDLA loading from 5 to 20 wt %. It should be noted that the increase in E' is significant with the PDLA loadings of 20 wt % at temperature above the glass state (80–90°C),

Applied Polymer SCIENCE

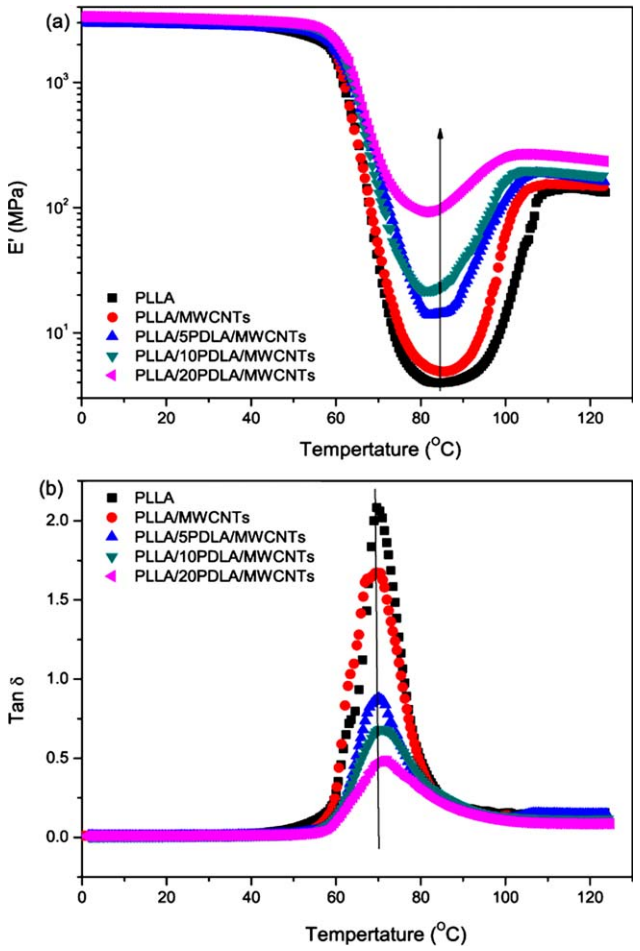

Figure 8. Temperature dependence of (a) E' and (b) tan δ for neat PLLA and various nanocomposites. [Color figure can be viewed in the online issue, which is available at wileyonlinelibrary.com.]

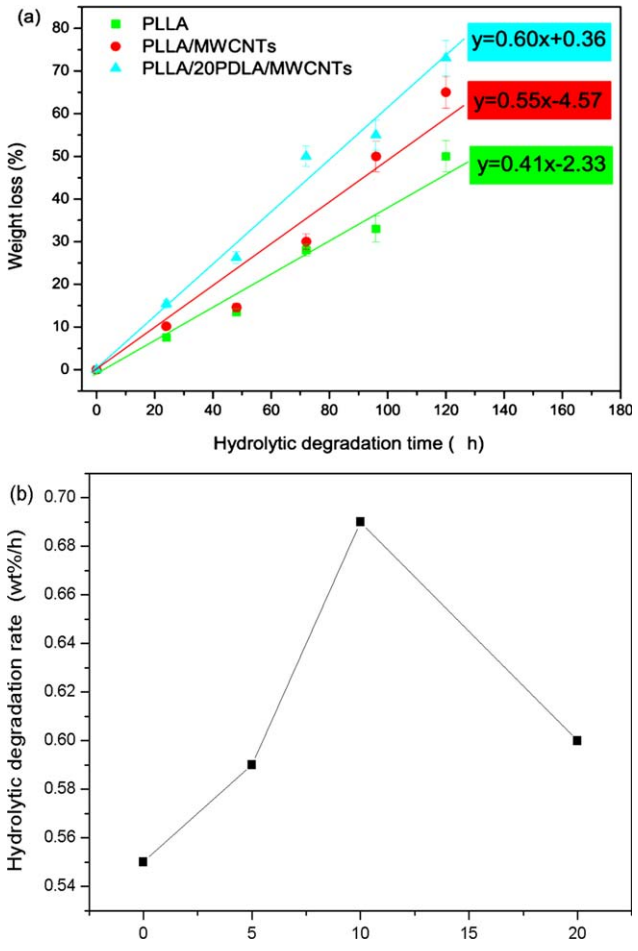

Figure 9. (a) Variation of weight loss with hydrolytic degradation time for neat PLLA and various nanocomposites; (b) hydrolytic degradation rates as a function of PDLA content for various nanocomposites. [Color figure can be viewed in the online issue, which is available at wileyonlinelibrary.com.]

indicating that the reinforcement effect of the PDLA loadings on E' is more pronounced at higher PDLA content. The significant improvement in E' may be ascribed to the effect of high performance of *in situ* formed stereocomplex crystals. Above T_g, when materials become soft, the reinforcement effect of the stereocomplex crystals on the matrix becomes prominent and hence strong enhancement of modulus can be observed. Furthermore, at the temperature range below the glass state (0–60°C), the increment in E' are about 15% for PLLA/MWCNTs nanocomposites, compared to that of pure PLLA. This is due to the mechanistic reinforcement by the MWCNTs. However, no significant change of the corresponding E' for the PLLA/PDLA/MWCNTs nanocomposites with PDLA content was observed, compared to that of PLLA/MWCNTs nanocomposites. From Figure 8(b), the T_g for both neat PLLA and the PLLA/MWCNTs nanocomposites are estimated to be around 69°C, indicating that the presence of MWCNTs does not significantly influence the segmental motion of PLLA in the nanocomposites. The slightly enhancement of T_g for PLLA/PDLA/MWCNTs nanocomposites may be due to the fact that PLLA homopolymer chains can possibly become tethered to or even come between stereocomplex crystals, thus reducing chain mobility.

Hydrolytic Degradation

Figure 9(a) shows the variation of weight loss of neat PLLA, PLLA/MWCNTs, and PLLA/PDLA/MWCNTs nanocomposites with exposed time during hydrolysis test. The values of weight loss increase with prolonging exposed time for all samples. As shown in Figure 9(a), mass loss starts from the beginning of each degradation experiment and shows almost linear variation of weight loss with exposed time until 120 h. Since the weight loss shows almost linear increase with hydrolytic degradation time, the hydrolytic degradation rates of neat PLLA, PLLA/MWCNTs, and PLLA/PDLA/MWCNTs nanocomposites are obtained from the slopes of the plots of variation of weight loss with hydrolytic degradation time. Figure 9(b) shows hydrolytic degradation rates as a function of PDLA content for various nanocomposites. For neat PLLA and PLLA/MWCNTs, the hydrolytic degradation rates are around 0.41wt %/h and 0.55wt %/h, respectively. The results that PLLA degrades faster in the PLLA/MWCNTs nanocomposites than in neat PLLA have also been recently reported in the literature. Qiu et al. have reported that the hydrolytic degradation of the PLLA composites containing MWCNTs was faster than those of neat PLLA.[22] It should be noted that the hydrolytic degradation rates are increased to be around 0.59, 0.69, and 0.6 wt

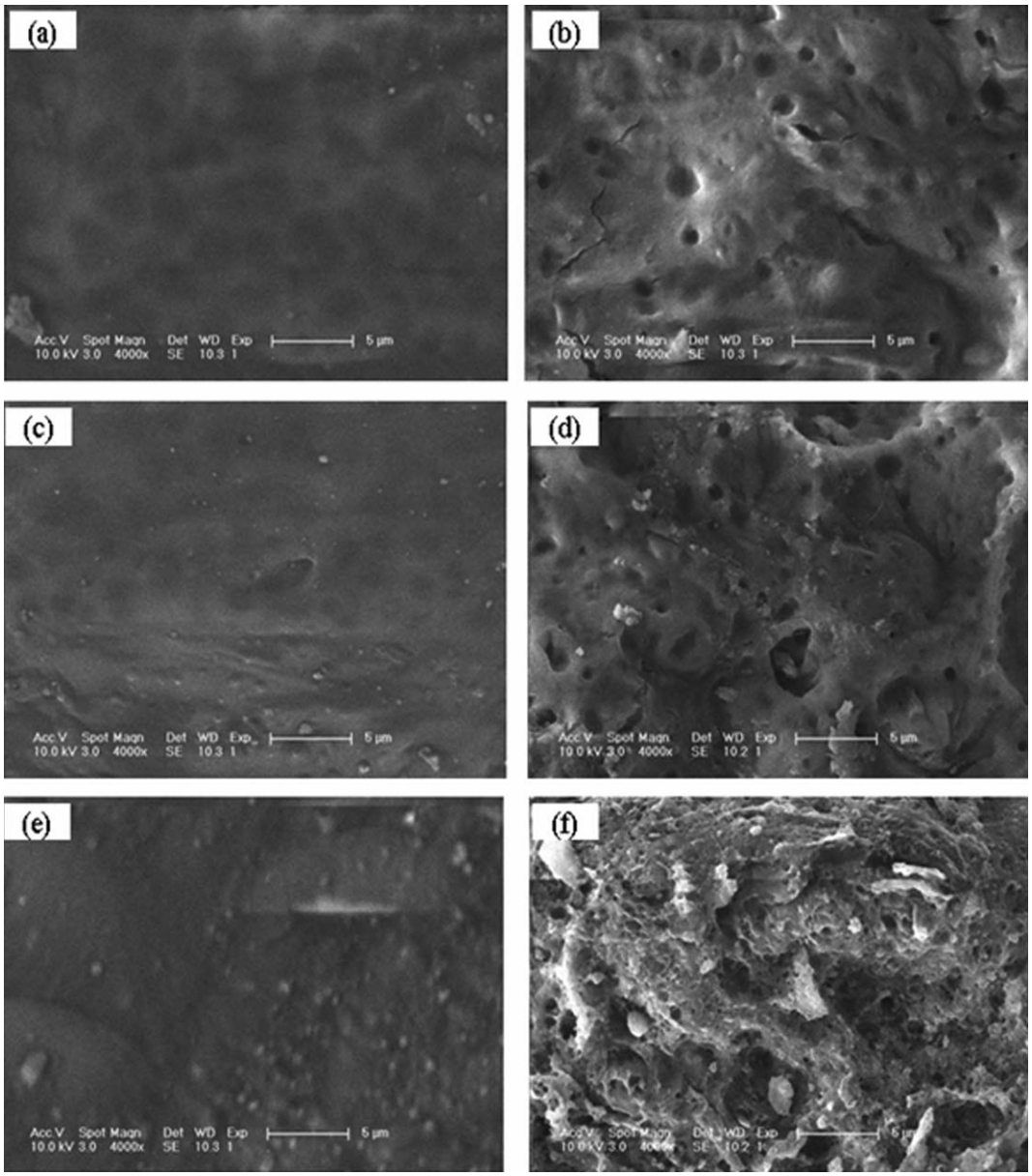

Figure 10. ESEM images showing the morphology of surface before hydrolytic degradation for (a) neat PLLA, (c) PLLA/MWCNTs, and (e) PLLA/PDLA20/MWCNTs and after hydrolytic degradation of 48 h for (b) neat PLLA, (d) PLLA/MWCNTs, and (f) PLLA/PDLA20/MWCNTs.

%/h for the PLLA/PDLA/MWCNTs nanocomposites with increasing the PDLA loading from 5 to 20 wt %. Figure 10 shows FESEM images of the morphology of surface before and after hydrolytic degradation for various samples. It is obvious that the PLLA/PDLA/MWCNTs nanocomposites degrade faster than PLLA/MWCNTs nanocomposite, indicating the loading of PDLA accelerates the hydrolytic degradation of PLLA/MWCNTs nanocomposite; moreover, the hydrolytic degradation rate increases with increasing the PDLA content up to 10 wt % and then decreases with further increasing the PDLA loading and exhibits the maximum value in the PLLA/PDLA10/MWCNTs sample.

The interesting and exciting aspect of this research is the enhanced hydrolytic degradation of PLLA/MWCNTs nanocomposites after incorporation of PDLA as evidenced from the aforementioned results. It is well known that two kinds of factors affect the degradation of aliphatic polyesters. One is various external environmental factors such as pH, temperature, and relatively humidity. The other is internal factors such as molecular weight, branched structure, crosslinking, and degree of crystallinity.[35,36] In this work, the same environmental conditions were used in studying the hydrolytic degradation. Moreover, one may argue that the improved dispersion of MWCNTs (as seen from Figure 3) seems to be an important contributing factor in giving rise to the significantly enhanced hydrolytic degradation rate of PLLA/PDLA/MWCNTs nanocomposite. However, this assumption as a key contributor can be easily

ruled out. For the samples containing 5 wt% and 10 wt% PDLA, the dispersion of MWCNTs is similar; however, the hydrolytic degradation rate is different. Therefore, the substantial difference in the hydrolytic degradation rate among these nanocomposites should mainly depend on the loading of PDLA and *in situ* formed stereocomplex crystals. It is important to discuss how the loading of PDLA and stereocomplex formation may influence the hydrolytic degradation. First, stereocomplex crystals may act as dispersed solid particles in the melt. In this case, the solid particulates may be stereocomplex lamellae or more complex spherulitic structures comprising some amorphous material as well.[18] The stereocomplex crystals showed high hydrolysis resistance.[13] During hydrolysis process, most of the amorphous chains were hydrolyzed and removed, while stereocomplex crystals were left alone. It seems that stereocomplex crystals with spherulitic structures can be released from the film surface, thus leading to form more porous structure, which accelerates the hydrolysis degradation.[37] Moreover, the M_w of PDLA (110,000) is lower than that of PLLA (207,000). The pending segments of the chains of PDLA that do not participate in the stereocomplex formation may be easier to hydrolyze compared with that of neat PLLA. All these factors may contribute to the enhanced hydrolytic degradation of PLLA/PDLA/MWCNTs nanocomposites. Moreover, when the PDLA content is up to 20 wt%, a three-dimensional network structure through physical cross-links by stereocomplex formation between multiple chains may be formed.[12] PLLA homopolymer chains may be tethered at multiple junctures, which leads to the decreased hydrolytic degradation rate of PLLA/PDLA20/MWCNTs sample compared with PLLA/PDLA5/MWCNTs and PLLA/PDLA10/MWCNTs samples. The exact degradation mechanism of PLLA/PDLA/MWCNTs nanocomposites is still unclear and needs further investigation. In brief, PLLA/MWCNTs nanocomposites preparation with PDLA enhances the hydrolytic degradation, which may be of great interest for its wide practical application.

CONCLUSIONS

Biodegradable PLLA/PDLA/MWCNTs nanocomposites were prepared successfully in this work via simple melt compounding at various PDLA loadings. Scanning electron microscopy observation indicated that MWCNTs were nicely dispersed in the PLLA/PDLA/MWCNTs ternary blends with 20 wt % PDLA loading due to the increase shear stress. Isothermal melt crystallization kinetics of neat PLLA and its various nanocomposites was studied with DSC at various crystallization temperatures and analyzed by the Avrami equation. The overall crystallization rates are faster in the PLLA/PDLA/MWCNTs nanocomposites than in PLLA/MWCNTs nanocomposite; however, the crystallization mechanism remains unchanged despite the presence of PDLA. The POM results show that the number of PLLA spherulites is greater in the PLLA/PDLA/MWCNTs nanocomposites than in PLLA/MWCNTs nanocomposite; moreover, the size of PLLA spherulites is smaller in the PLLA/PDLA/MWCNTs nanocomposites than in PLLA/MWCNTs nanocomposite. The increased nucleation density of PLLA spherulites in the nanocomposites indicates that stereocomplex crystals formed *in situ* may act as an effective nucleating agent during the crystallization process of PLLA/MWCNTs nanocomposite. On the basis of the WAXD study, it can be concluded that the incorporation of PDLA does not modify the crystal structure of PLLA in the nanocomposites relative to PLLA/MWCNTs nanocomposite. The E' has been apparently improved in the PLLA/PDLA/MWCNTs, while the T_g varied slightly among neat PLLA, the PLLA/MWCNTs, and PLLA/PDLA/MWCNTs nanocomposites. The exciting result of this work is that the hydrolytic degradation rates have been enhanced obviously in the PLLA/PDLA/MWCNTs nanocomposites than PLLA/MWCNTs nanocomposites, which may be of great use and importance for the wider practical application of PLLA/MWCNTs nanocomposites.

ACKNOWLEDGMENTS

This work is supported by the National Science Foundation of China (50703042). Part of this work is supported by Jilin Province Science and Technology Agency (20116025) and Jilin Jianzhu University (862107).

REFERENCES

1. Garlotta, D. *Polym. Environ.* **2001**, *9*, 63.
2. Jiang, L.; Liu, B.; Zhang, J. *Ind. Eng. Chem. Res.* **2009**, *48*, 7594.
3. James, L. *Polym. Degrad. Stab.* **1998**, *59*, 145.
4. Pan, H.; Qiu, Z. *Macromolecules* **2010**, *43*, 1499.
5. Ray, S. S. *Acc. Chem. Res.* **2012**, *45*, 1710.
6. Södergård, A.; Stolt, M. *Prog. Polym. Sci.* **2002**, *27*, 1123.
7. Ikada, Y.; Jamshidi, K.; Tsuji, H.; Hyon, S. *Macromolecules* **1987**, *20*, 906.
8. Tsuji, H. *Macromol. Biosci.* **2005**, *5*, 569.
9. Yamane, H.; Sasai, K. *Polymer* **2003**, *44*, 2569.
10. Rahman, N.; Kawai, T.; Matsuba, G.; Nishida, K.; Kanaya, T.; Watanabe, H.; Okamoto, H.; Kato, M.; Usuki, A.; Matsuda, M.; Nakajima, K.; Honma, N. *Macromolecules* **2009**, *42*, 4739.
11. Nousilhas, H.; Li, F.; Ghzaoui, A.; Li, S.; Coudane, *J. Polym. Int.* **2010**, *59*, 1077.
12. Schmidt, S.; Hillmyer, M. *J. Polym. Sci. Part B: Polym. Phys.* **2001**, *39*, 300.
13. Ndersson, S.; Hakkarainen, M.; Inkinen, S.; Södergård, A.; Albertsson, A. *Biomacromolecules* **2010**, *11*, 1067.
14. Sun, Y.; He, C. *ACS Macro. Lett.* **2012**, *1*, 709.
15. Woo, E.; Chang, L. *Polymer* **2012**, *52*, 6080.
16. Anderson, K.; Hillmyer, M. *Polymer* **2006**, *47*, 2030.
17. Quan, H.; Zhang, S. J.; Qiao, J. L.; Zhang, L. Y. *Polymer* **2012**, *53*, 4547.
18. Saeidlou, S.; Huneault, M. A.; Li, H. B.; Sammut, P.; Park, C. B. *Polymer* **2012**, *53*, 5816.
19. Li, Y.; Han, C. Y. *Ind. Eng. Chem. Res.* **2012**, *51*, 15927.
20. Krikorian, V.; Pochan, D. J. *Chem. Mater.* **2003**, *15*, 4317.

21. Bian, J. J.; Han, L. J.; Wang, X. M.; Wen, X.; Han, C. Y.; Wang, S. S.; Dong, L. S. *J. Appl. Polym. Sci.* **2010**, *116*, 902.
22. Zhao, Y. Y.; Qiu, Z. B.; Yang, W. T. *J. Phys. Chem. B* **2008**, *112*, 16461.
23. Pan, H.; Qiu, Z. B. *Macromolecules* **2010**, *43*, 1499.
24. Moon, S.; Jin, F. Z.; Lee, C. J.; Tsutsumi, S.; Hyon, S. H. *Macromol. Symp.* **2005**, *224*, 287.
25. Zhang, D. H.; Kandadai, M. A.; Cech, J.; Roth, S.; Curran, S. A. *J. Phys. Chem. B* **2006**, *110*, 12910-12915.
26. Wu, C. S.; Liao, H. T. *Polymer* **2007**, *48*, 4449.
27. Chen, G. X.; Shimizu, H. *Polymer* **2008**, *48*, 943.
28. Li, Y. J.; Shimizu, H. *Polymer* **2007**, *47*, 2203.
29. Avrami, M. *J. Chem. Phys.* **1940**, *8*, 212.
30. Avrami, M. *J. Chem. Phys.* **1941**, *9*, 177.
31. Pan, P. J.; Inoue, Y. *Prog. Polym. Sci.* **2009**, *34*, 605.
32. Pan, P.; Zhu, B.; Kai, W.; Dong, T.; Inoue, Y. *Macromolecules* **2008**, *41*, 4296.
33. Di Lorenzo, M. *Eur. Polym. J.* **2005**, *41*, 569.
34. Ray, S. S.; Yamadab, K.; Okamotoa, M.; Ueda, K. *Polymer* **2003**, *44*, 857.
35. Han, C. Y.; Bian, J. J.; Hao, L.; Han, L. J.; Wang, S. S.; Dong, L. S.; Chen, S. *Polym. Int.* **2010**, *59*, 695.
36. Numata, K.; Wistrand, A.; Albertsson, A.; Doi, Y.; Abe, H. *Biomacromolecules* **2008**, *8*, 2180.
37. Tsuji, H.; Kawashima, Y.; Takikawa, H.; Saburo, T. S. *Polymer* **2007**, *48*, 4213.